Pressure-induced *f*-electron delocalization in the U-based strongly correlated compounds UPd_3 and UPd_2Al_3: Resonant inelastic x-ray scattering and first-principles calculations

J.-P. Rueff,[1,2] S. Raymond,[3] A. Yaresko,[4] D. Braithwaite,[3] Ph. Leininger,[2] G. Vankó,[5] A. Huxley,[3] J. Rebizant,[6] and N. Sato[7]

[1]*Synchrotron SOLEIL, L'Orme des Merisiers, Saint-Aubin, Boîte Postale 48, 91192 Gif-sur-Yvette Cedex, France*

[2]*Laboratoire de Chimie Physique-Matière et Rayonnement, CNRS, Université Pierre et Marie Curie, 75005 Paris, France*

[3]*CEA-Grenoble, DRFMC/SPSMS, 38054 Grenoble Cedex, France*

[4]*Max-Planck-Institut für Physik komplexer Systeme, Nöthnitzer Straße 38, 01187 Dresden, Germany*

[5]*European Synchrotron Radiation Facility, Boîte Postale 220, F-38043 Grenoble Cedex 9, France*

[6]*European Commission, Institute for Transuranium Elements, Postfach 2340, D-76125 Karlsruhe, Germany*

[7]*Physics Department, Tohoku University, Sendai 980-8578, Japan*

(Received 19 March 2007; revised manuscript received 25 May 2007; published 10 August 2007)

We have measured the uranium L_3 absorption and resonant emission spectra in the localized magnetic compound UPd_3 and heavy fermion UPd_2Al_3 as a function of pressure. The spectral line shape of the absorption edge is found to vary rapidly in UPd_2Al_3 with a notable broadening of the white line above the structural transition around 25 GPa while it shows a more gradual variation in UPd_3 over the considered pressure range (0–40 GPa), indicating different responses of the *f*-*d* electrons to the compressed lattice in the two compounds. The U L_3 absorption spectra in both UPd_3 and UPd_2Al_3 and their pressure dependence were further simulated via first-principles band calculations within the linear muffin-tin orbital approach. The calculations reproduce the main features of the experimental absorption edges. The calculated pressure dependence of the *f* charge reveals a stronger localization of the *f* electrons in UPd_3 which shows a remarkably stable valency under pressure, close the nominal value of 4. On the contrary, our results point to a mixed valent $U^{4-\delta}$ ground state in UPd_2Al_3 at ambient conditions, evolving into a U^{4+} (or possibly $U^{4+\delta}$) configuration at high pressure. The *f*-electron delocalization could be responsible for the known structural transition in UPd_2Al_3.

DOI: 10.1103/PhysRevB.76.085113 PACS number(s): 71.20.Eh, 71.27.+a, 78.70.Dm, 71.15.−m

I. INTRODUCTION

Most of the recent interest in the physics of heavy fermion compound stems from the occurrence of unconventional superconductivity and marginal Fermi liquid behavior.[1] These phenomena are intimately connected to quantum critical phenomena that correspond to the disappearance of a magnetic ordered phase at $T=0$ K as a function of a nonthermal parameter, *r*: pressure (*P*), chemical composition (*x*), or magnetic field (*H*). In the ordered state, the valence configuration of the ion underlies a magnetic ground state that corresponds in the simplest cases to a Kramers doublet. However, the ionic configuration can be altered by charge fluctuations that are well known to be responsible for producing the intermediate valence phenomena in other regions of the (*T*-*r*) phase diagram. Such effects may not be negligible even in the vicinity of the quantum critical point. This is exemplified by the enhancement of the superconducting temperature in $CeCu_2Si_2$ at the pressure where charge fluctuations are strongest[2] and also by the occurrence of noninteger valence in the magnetic phase of SmS.[3,4] It thus turns out that for the complete understanding of these strongly correlated electron systems, not only the low lying excitations must be understood but also the higher energy ones that allow us to understand how the ground state is constructed from a series of characteristic higher level energies: hybridization, crystal field, spin-orbit and Coulomb interactions.

In this framework, the valence properties of 4*f*-electron systems were recently studied by resonant inelastic x-ray scattering (RIXS) techniques.[5–8] This second-order spectroscopy involves the absorption of an incident photon in the vicinity of a resonance and emission of a secondary photon. Because a core electron is involved, the process is selective of the probed atomic shell and orbital. In intermediate valent systems, the ground state can be formally written as a superposition of two or more pure-valent configurations. When a core hole is created, such as in the x-ray absorption spectroscopy (XAS) and x-ray photoemission spectroscopy (XPS) final states, the ground state degeneracy is lifted out and one can in principle proceed to a counting of the *f* electrons. The picture is in reality complicated by the conspicuous mixing of states occurring in the XPS or XAS final states in the presence of the core hole. This ultimately precludes a reliable description of the valent state properties. Compared to first-order spectroscopies, RIXS advantageously provides a fine tuning of the intermediate and final states involved, through the choice of the incident and emitted energies E_1 and E_2. Owing to the resonant process, specific states of given symmetry can be enhanced and separately studied. The gains in terms of spectral analysis supplied by RIXS have proven to be extremely effective to address intermediate valence issues in strongly correlated materials. In addition, as an all-photon spectroscopy, RIXS in the hard x-ray range is well adapted to system material under high pressure conditions.[9–12]

In the present work, we extend the investigation of *f*-electron materials under pressure to 5*f* uranium compounds. Due to the hierarchy between crystal field and spin-orbit interactions, the 5*f* electrons are intermediate between the 4*f* and the 3*d* electrons in terms of localization.[13] Moreover, the 5*f* electron bandwidth, the spin-orbit energy, and

the on-site Coulomb repulsion are generally of the same magnitude and must be taken into account on the same footing. For many cases, the valence is unknown and the two configurations U^{3+} ($5f^3$, $J=9/2$) and U^{4+} ($5f^2$, $J=4$) are usually considered. One difficulty to distinguish between these two states is that they have very similar paramagnetic moment. It is thus of interest to apply the RIXS method that is known to be an efficient way to determine the valence of rare earth based compounds to their $5f$ counterparts. To this purpose, we have selected relevant examples in that context (UPd_3, UPt_3, and UPd_2Al_3) which are expected to exhibit contrasted $5f$ localization behaviors. In addition, two of these compounds (UPd_3 and UPd_2Al_3) have been put under external pressure with the aim to further change their valence. UPd_3 is a rare clear case of a well defined $5f^2$ localized state, evidenced through the measurement of crystal field excitations by neutron spectroscopy.[14] This was later confirmed in photoemission experiments by the finding that the f states are located well below the Fermi level.[15] Pressure-induced delocalization toward a $5f^1$ state was predicted by self-interaction corrected (SIC) local spin density (LSD) calculation and is expected at about 25 GPa.[16] SIC-LSD method allows f electrons to have both localized and delocalized characters to deal with mixed valent materials.[17] However, in UPd_3 no corresponding effect of volume collapse was experimentally observed up to 53 GPa in x-ray diffraction under pressure.[18] The second compound UPt_3 is an archetypical heavy fermion unconventional superconductor ($T_c=0.5$ K).[1] Contrarily to UPd_3, $5f$ weight was observed in photoemission experiment at the Fermi level.[19] It is proposed that the coupling between localized f^2 electrons and delocalized f electron is at the origin of the part of the heavy fermion behavior of this compound.[20] The last example UPd_2Al_3 is an antiferromagnetic superconductor ($T_N=14$ K, $T_c=2$ K) with well characterized interplay between magnetism and superconductivity.[1] A dual nature of the f electrons is also proposed in UPd_2Al_3.[21] In this compound, a structural phase transition occurs under pressure and the corresponding doubling of the compressibility was related to a valence change.[22]

The experimental work is described in a first part. The data obtained by a RIXS-derived technique [x-ray absorption in the partial fluorescence yield (PFY-XAS)] are presented in Sec. II in UPd_3 and UPd_2Al_3 under pressure and UPt_3. The variation of the electronic properties under pressure is analyzed within a first-principles approach in the linear muffin-tin orbital (LMTO) method in Sec. III. The results are discussed in terms of f-electron delocalization in Sec. IV, before drawing the concluding remarks in Sec. V.

II. EXPERIMENT

A. Partial fluorescence yield absorption

The experiment was carried out at ID-16 at the European Synchrotron Radiation Facility (ESRF) using the beamline Raman spectrometer. The beam was monochromatized by a pair of Si(111) crystals and focused in a 50×140 μm^2 spot at the sample position by a toroidal mirror located downstream. The spectrometer was equipped with a spherically bent Ge(777) analyzer and an avalanche photodiode detector in the Rowland circle geometry with 1 m radius. The total energy resolution was estimated at 2.1 eV by measuring the quasielastic line full width at half maximum (FWHM) at 13.6 keV. The monochromator resolution at 13.6 keV (17 keV) is estimated at 1.8 eV (2.0 eV), while the analyzer gives rise to an additional contribution of ~0.5 eV at the nominal Bragg angle of 77.68°. The samples were loaded in a membrane pressure cell with a 16:4:1 methanol-ethanol-water mixture as the pressure transmitting medium. The medium is strictly hydrostatic up to the freezing pressure P_f (~14 GPa) but remains quasihydrostatic well above P_f; the estimated differential stress at 25 GPa is about 0.15 GPa.[23]

We used single crystals of UPd_3, UPt_3, and UPd_2Al_3 taken from the same batch as in Refs. 18, 24, and 25, respectively. The crystals were cut prior to loading in order to match the gasket hole diameter (150 μm) with a thickness (~20 μm) which is adequate for measurements in transmission geometry at 13.6 keV.

Figure 1(a) shows the XAS spectra measured in UPd_3 at the U L_3 ($2p\rightarrow5d$ transition) edge as a function of pressure. The spectrum obtained in UPt_3 at ambient pressure is also displayed as element of comparison. The absorption spectra were acquired in the partial fluorescence yield (PFY) mode by monitoring the intensity of the U $L\alpha_1$ emission line ($3d\rightarrow2p$ transition) at 13.61 keV, as the incident energy is swept across the L_3 edge. The zero energy was taken at the inflection point of the white line, located at 17.174 keV. As shown extensively in previous studies,[26–28] the PFY method provides absorption spectra partially free from the core-lifetime broadening effects. Although there is no strict equivalence with conventional XAS,[29] compared to the latter, the PFY spectra do show improved resolution mostly evident in the preedge region, where the dipolar tail is strongly suppressed. The gain of intrinsic resolution is particularly appreciable in the case of uranium: the U $2p$ core-hole lifetime [~7.4 eV (Ref. 30)] is more than a factor 2 larger than that of the U $3d$ core hole estimated at 3.3 eV.[31] Figures 1(c) and 1(d) show a comparison in UPd_3 and UPd_2Al_3 between the absorption spectra measured in the total fluorescence yield (TFY) and PFY modes at ambient conditions. The TFY spectra were acquired with a *PIN* diode simultaneously to the PFY measurements and are normalized in Fig. 1 to the same step height at the absorption edge. The spectral sharpening is of particular interest to reveal masked features below the edge such as excited states in intermediate valent f-electron systems.[8,9]

In UPd_3, the uranium PFY-L_3 spectrum is composed of an intense white line (A) and high-energy features somewhat broader in energy which extend up to 40 eV above the edge (C, D, and D'). No structure can be observed in the preedge region. As pressure increases, the structure C gains in intensity while the high-energy features D and D' seemingly split in energy. Simultaneously, a shoulder A' appears on the low energy side of the white line that gradually becomes asymmetric, followed by a weak hump (B) that seems to grow in intensity.

The evolution of the U L_3 edge in UPd_2Al_3 as a function of pressure, illustrated in Fig. 1(b), differs in many ways

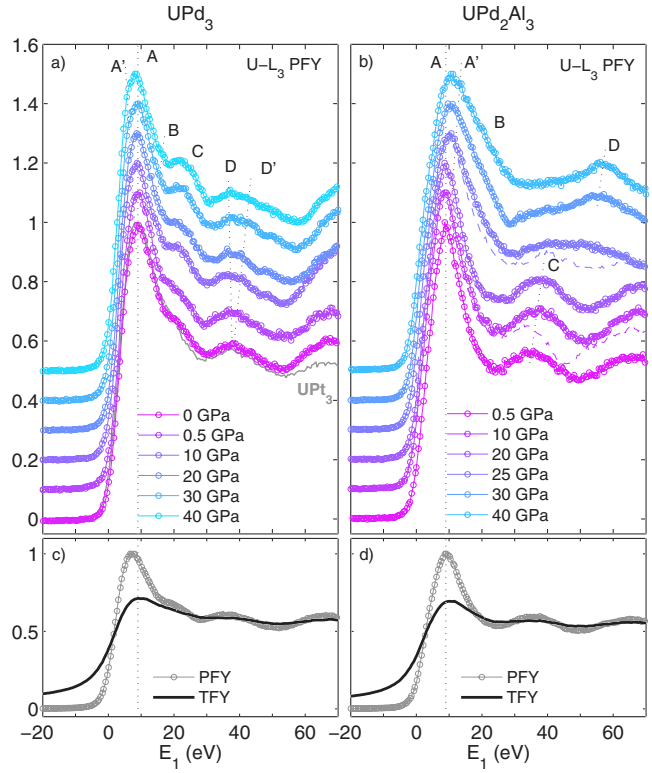

FIG. 1. (Color online) U L_3 partial fluorescence yield absorption spectra in (a) UPd_3 and (b) UPd_2Al_3. Dashed lines in panel (b) denote spectra measured upon pressure release (at 25 and 10 GPa). The spectrum obtained at ambient pressure in UPt_3 is also shown [panel (a)] (solid line). Dotted lines are guide to the eyes. Comparison between partial fluorescence yield (PFY) (open circles) and total fluorescence yield (TFY) (thick solid lines) modes is presented in panels (c) and (d), respectively, for UPd_3 and UPd_2Al_3 at ambient conditions.

from the behavior in UPd_3. At low pressure, the spectra are characterized by a white line (A) relatively narrow compared to UPd_3, followed by a well resolved structure (C) located at ~30 eV above the edge. The spectra show nearly no changes up to 20 GPa except for the progressive increase of a second feature which appears as a shoulder to the white line (A') along with a slight energy shift of the white line itself A and of the high-energy oscillations C. This underlies that nonhydrostaticity is not an issue here, as far as the electronic properties are concerned. At higher pressure, a dramatic transformation occurs in the spectral line shape when passing the structural transition pressure reported at around 23.5 GPa.[22] The white line suddenly broadens, while the high-energy oscillating pattern reduces to a single peak (D). Note that the spectrum at 25 GPa is somehow intermediate between the two regimes. The spectra measured upon pressure release [dashed lines in Fig. 1(b)] confirm that the structural change is essentially reversible (with some hysteresis), although we notice a distortion of the 10 GPa spectrum, especially in the high-energy region.

For completeness of information, we have also measured the resonant U $L\alpha$ emission line as a function of the incident energy E_1 through the U L_3 absorption edge, a method referred to as the $2p3d$ resonant x-ray emission spectroscopy (RXES). Contrary to what is observed in Ce or Yb compounds, the RXES spectra in the uranium compounds (not shown) are rather featureless and do not reveal any spectral components related to the intermediate uranium valence state. In rare earth, $2p3d$ RXES is able to resolve additional f^n components of the mixed ground state which are not seen in the absorption spectra. This is not the case in uranium where the relevant lifetimes and bandwidths are much larger than in the $4f$ elements. Hence, despite the sharpening effect inherent to the RXES process, the spectra are still dominated by broadening effects related to the width of the $6d$ band, significantly larger than the respective $5d$ band in rare earth.

Clearly enough, the experimental data obtained in the uranium compounds have no straightforward interpretation in terms of valence change. Hints about the uranium electronic properties under pressure, however, can be gained by simulation of the U L_3 spectra by first-principles calculations within the LMTO approach. In UPd_3, this method has proven to give a pertinent solution with two localized f electrons,[32] while the $5f$ level in UPt_3 are found partly delocalized in agreement with the XPS results. The method is here applied to the absorption spectra in UPd_2Al_3 and UPd_3 under pressure.

III. CALCULATIONS

The calculations of the electronic band structure and U L_3 absorption spectra were performed within the local density approximation (LDA) using the relativistic LMTO method in the atomic sphere approximation (ASA).

U L_3 absorption spectra were calculated in the dipole approximation and broadened using a Lorentzian of FWHM γ=3.0 eV and a Gaussian of γ=1.0 eV which account for the core-hole lifetime and the experimental resolution, respectively. The spectra are normalized so that the intensity of the main peak is equal to 1. No attempt was made to reproduce the continuum (usually by adding *atan*-like contribution) as we mostly focus on the pressure dependence of the peak positions and not on the intensity change.

A. UPd_3

The uranium L_3 XAS spectra in UPd_3 calculated for the dhcp ($P6_3/mmc$) structure are shown in Fig. 2. The a and c lattice parameters were borrowed from Ref. 18 for all the considered pressure points in the range of 0–40 GPa. The zero energy is chosen at the absorption edge (the Fermi level) of the spectrum calculated for ambient pressure lattice constants. The spectra shown in the left panel of Fig. 2 are calculated with U $7s$, $7p$, $6d$, $5f$ and Pd $5s$, $5p$, $4d$, $4f$ muffin-tin (MT) orbitals included into the basis set. These theoretical spectra reproduce well the main features of the experimental spectra (Fig. 1) up to ~30 eV. Above this energy, however, the calculated XAS intensity rapidly decreases, whereas the experimental spectra show an upturn with a broad maximum located between 25 and 45 eV above the absorption edge. The reason for this discrepancy is that above ~15 eV, the d states in the uranium atomic sphere

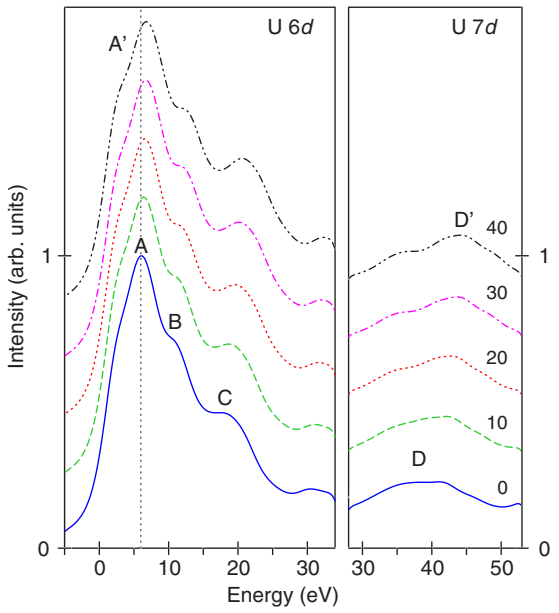

FIG. 2. (Color online) Calculated pressure dependence of the U L_3 XAS spectra in UPd_3. The spectra are normalized to a height of 1 and a vertical offset of 0.2 is added. Zero energy is chosen at the absorption edge of the spectrum calculated for ambient pressure lattice constants. The calculations in the left and right panels are performed with different basis sets (see text for details).

(AS) acquire an additional node and it is necessary to include into the LMTO basis the U 7*d* states instead of the U 6*d* ones in order to reproduce experimental XAS spectra above 30 eV. The latter are centered at ~40 eV and span over the energy range of 30–60 eV. We have found that in order to describe properly the hybridization of the U 7*d* states above 45 eV, the basis should be extended with U and Pd 5*g* states. Also, Pd 5*d* and U 6*f* MT orbitals, which lie in the same energy range, were included into the basis instead of Pd 4*d* and U 5*f*, respectively. XAS spectra calculated with this basis set are shown in the right panel of Fig. 2.

The theoretical spectra show four features marked by *A*, *B*, *C*, and *D* in Fig. 2. The origin of the first three of them can be clarified by comparing the U 6*d* density of states (DOS) to the *l*-projected densities of Pd states shown in Fig. 3. The main peak (*A*) with the maximum at 6 eV at ambient pressure is formed by transitions to unoccupied U 6*d* states extending from the Fermi level (E_F) to ~10 eV above it. Due to strong U *d*-U *d* and U *d*-Pd *d* hybridizations, the structure of the densities of 6*d* states of two inequivalent uranium ions in this energy range is rather complex. It consists of a prominent peak at ~2.5 eV and a number of peaks of decreasing heights above 4 eV. However, after broadening of the calculated L_3 spectra and summation of the contributions from two uranium ions, the DOS structures appear smeared out and the peak at 2.5 eV manifests itself only as a shoulder (A') at the low energy slope of the main peak. Lattice compression under pressure causes the increase of the width of U *d* states. As a result, the maximum of peak *A* shifts by 0.8 eV to higher energies and the shoulder A' at the low energy slope becomes more pronounced.

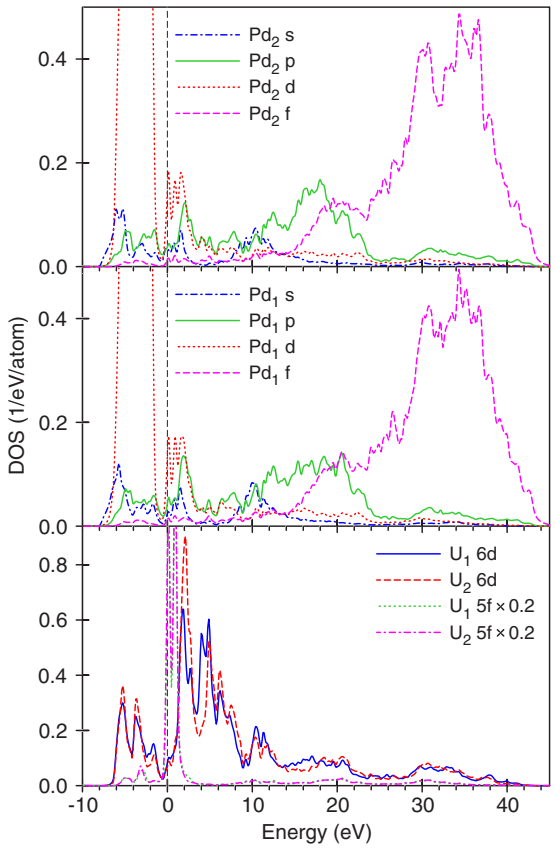

FIG. 3. (Color online) Site- and *l*-resolved densities of unoccupied states in UPd_3 calculated for the ambient pressure lattice parameters. Subscript refers to the calculations for the two inequivalent U sites. For uranium, only the 6*d* and 5*f* DOS are shown. The U 5*f* DOS is multiplied by a factor of 0.2.

A peak between 10 and 12 eV in the U *d* DOS is responsible for feature *B* in the theoretical L_3 spectra. The corresponding U *d* states hybridize with delocalized Pd 5*s* states and feature *B* shows stronger pressure dependence than the *A* peak, with the shift to higher energies being ~1.8 eV at 40 GPa. The pressure evolution of this feature may explain the appearance of a small hump at the high-energy slope of the main peak in the experimental spectra at high pressures. Above ~13 eV, the shape of the U *d* DOS reproduces the energy dependence of the density of free-electron-like Pd 5*p* states. A high-energy shift of the latter under pressure causes the shift of a broad peak of the U *d* DOS centered at 20 eV and of the corresponding peak *C* in the L_3 spectrum from 18 eV at ambient pressure to 20.5 eV at 40 GPa. This pressure dependence correlates with the behavior of the broad shoulder *C* in the experimental spectrum which under pressure of 40 GPa transforms into a well defined peak. Peak *D* in the calculated L_3 spectrum, which reflects the evolution of the U 6*d* states, also shows a shift of 2 eV to higher energies under pressure. This peak can be associated with the broad peak *D* in the experimental spectra.

Comparing the pressure dependence of the calculated and experimental U L_3 spectra in UPd_3, one can conclude that the calculations reproduce the increase of the width of the main peak *A* and the shift of peaks *C* and *D* to higher energies under pressure.

B. UPd_2Al_3

Relativistic LDA calculations for the low pressure phase ($P \leqslant 23.5$ GPa) of UPd_2Al_3 were performed using the experimental a and c lattice parameters in the $P6/mmm$ structure.[22] According to the x-ray diffraction study of Ref. 22, UPd_2Al_3 undergoes a structural phase transition to an orthorhombic high pressure (HP) phase of $Pmmm$ symmetry above the critical pressure $P_C \sim 23.5$ GPa. However, the refinement of the HP crystal structure was not successful. We carried out band structure calculations for the orthorhombic HP phase assuming a $Cmmm$ unit cell, thus neglecting the doubling of the unit cell in the c direction presumably responsible for the $Cmmm$ to $Pmmm$ symmetry lowering. U and Pd ions in the $Cmmm$ unit cell were placed into $2a$ (0,0,0) and $4i$ $(0,y,0)$ Wyckoff positions, respectively. Al ions were distributed over two inequivalent $2c$ $(0,1/2,1/2)$ and $4f$ $(1/4,1/4,1/2)$ sites. The $Cmmm$ structure is related to the undistorted $P6/mmm$ one by $\mathbf{a}_o=\mathbf{a}_h$, $\mathbf{b}_o=\mathbf{a}_h+2\mathbf{b}_h$, $\mathbf{c}_o=\mathbf{c}_h$, with $b_o=\sqrt{3}a_h$ and the only free atomic positional parameter y being equal to 1/3, where subscripts h and o are used for the hexagonal and orthorhombic structures, respectively. Since the exact position of Pd ions in the HP unit cell is not known in our calculations, y was fixed to the ideal value of 1/3. With y being fixed, the change of interatomic distances under pressure is uniquely determined by the change of a_o, b_o, and c_o lattice constants, for which the corresponding experimental values were used.[33]

The pressure dependence of calculated U L_3 XAS spectra in UPd_2Al_3 is shown in Fig. 4 with zero energy being chosen at the absorption edge of the ambient pressure spectrum. The absorption to the final states lying up to 30 eV above the Fermi level (left panel of Fig. 4) was calculated with the LMTO basis set containing U 7*s*, 7*p*, 6*d*, 5*f*, Pd 5*s*, 5*p*, 4*d*, 4*f*, and Al 3*s*, 3*p*, 3*d*, 4*f* states in the following denoted as LBS. XAS spectra presented in the right panel of Fig. 4 were calculated with U 7*d* and 6*f* states in the basis set which included also U and Pd 5*g* states (HBS). The extended basis set is denoted HBS. We found, however, that in contrast to UPd_3, XAS discussed in the previous section accounting for U and Pd 5*g* states has only a minor effect on the calculated U L_3 spectra.

The theoretical U L_3 spectra in UPd_2Al_3 are less structured compared to the corresponding UPd_3 spectra (Fig. 2). Below 30 eV, one distinguishes two main features: a symmetric peak *A* with a maximum at 5.5 eV at ambient pressure and a shoulder *B* at ~15 eV. The former is due to transitions into unoccupied U 6*d* states hybridized with Pd 4*d* and Al 3*p* states, while the latter can be related to a structure in U *d* DOS between 12 and 22 eV. This structure is present in the DOS curves calculated with U 6*d* as well as U 7*d* states included into the basis and follows the shape of Al 3*d* DOS (Fig. 5). Peak *C* in the right panel of Fig. 4 is formed by transitions into U 7*d* states.

As the lattice is compressed, hence simulating the effect of applying hydrostatic pressure, the width of the *A* peak increases and its maximum shifts slightly toward higher energies. These changes become more pronounced in the spectra calculated for the HP $Cmmm$ structure, for which at the pressure of 36.3 GPa a second maximum A' appears at

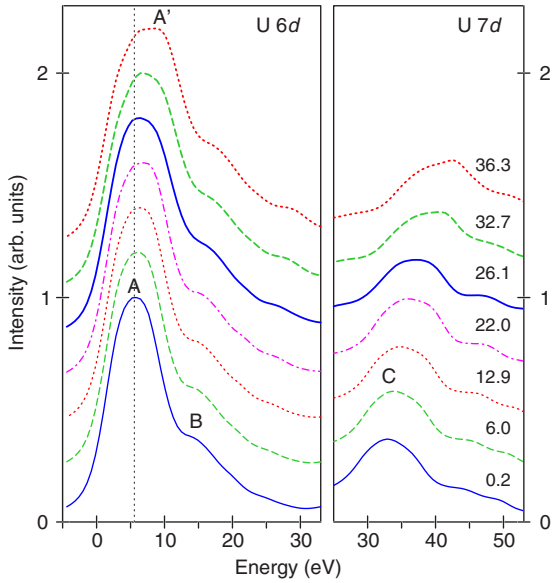

FIG. 4. (Color online) Calculated pressure dependence of the U L_3 XAS spectra in UPd_2Al_3. The spectra are normalized to a height of 1 and a vertical offset of 0.2 is added. Zero energy is chosen at the absorption edge of the spectrum calculated for ambient pressure lattice constants. The calculations in the left and right panels are performed with different basis set (see text for details).

9.3 eV. The *B* peak exhibits a high-energy shift of ~3 eV. The strongest pressure effect is observed for the *C* peak (right panel of Fig. 4) which shifts from 33 eV at zero pressure to 44 eV at 36.3 GPa and becomes more asymmetric.

In order to discriminate between the influence of the lattice compression and of the change of the crystal structure on the U L_3 spectra, we repeated calculations for $P \geq P_C$ using a hexagonal $P6/mmm$ unit cell with $a_h=(a_o b_o/\sqrt{3})^{1/2}$ and $c_h=c_o$, i.e., having the same volume as the corresponding orthorhombic one. The spectra calculated for the undistorted hexagonal structure show only minor differences from the spectra for the $Cmmm$ structure; the most noticeable one being a minor increase of the A' peak magnitude relative to *A*. Therefore, it seems that the greater sensitivity of the calculated U L_3 spectra to the pressure change above P_C is mainly due to the larger compressibility of the HP phase of UPd_2Al_3 as observed by x-ray diffraction.[22] The lowering of the lattice symmetry to the orthorhombic one and the corresponding splitting of the nearest neighbor distances play, at least within the structural model used in the present calculations, only a minor role in the formation of the XAS.

Comparing the pressure-induced changes of the experimental [Fig. 1(b)] and theoretical (Fig. 4) U L_3 XAS spectra, one can notice that the calculations reproduce reasonably well the evolution of the experimental spectra below P_C, in particular, the appearance of an additional feature A' at the high-energy slope of the main peak *A* and the appreciable shift of the *C* peak, which can be associated with the *C* peak in the calculated spectra, toward higher energies. However, the dramatic changes of the experimental spectra above the critical pressure (with the emergence of peak *D*) cannot be explained by our calculations.

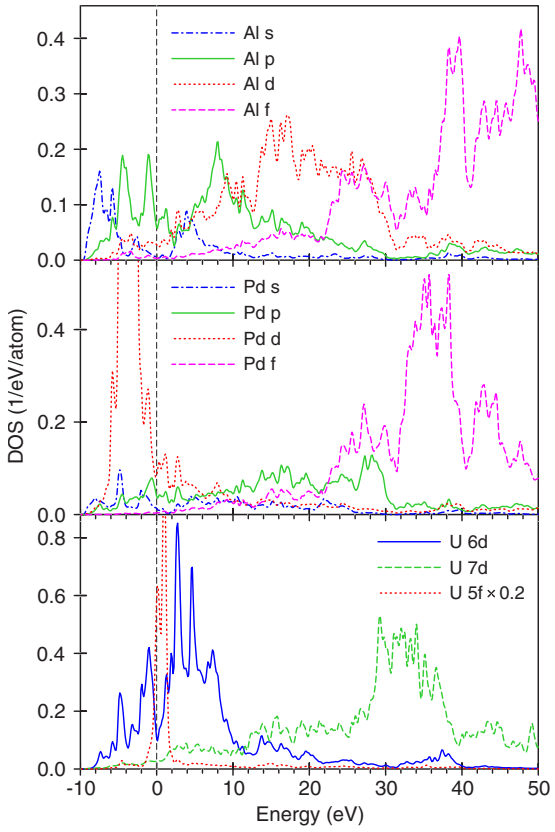

FIG. 5. (Color online) *l*-resolved densities of unoccupied states in UPd_2Al_3 calculated for the ambient pressure lattice parameters with LBS basis (see text). U 5*f* DOS is scaled down by a factor of 0.2. In the lower panel, the density of U 7*d* state obtained from the HBS calculation is plotted by a dashed line.

There are a number of possible reasons for this discrepancy. The calculations were performed within the local density approximation and, thus, cannot account for a many-body effects related to the possible change of the occupation of the U 5*f* states at P_C. However, the astonishing changes of the experimental spectra appear more than 25 eV above the absorption edge. Calculations show that the final states for XAS in this energy range are formed by U 7*d* states. It is difficult to believe that the reconstruction of U 5*f* shell and effects of $5f-7d$ Coulomb interaction can have so strong effect on the XAS spectra in this photon energy range. It seems more probable that the changes of the crystal structure at the critical pressure are much stronger than it is assumed by our structural model for the HP phase. This conclusion is also supported by the fact that for all $P > P_C$, the total energies calculated using the *Cmmm* unit cell are significantly higher than those obtained using the hexagonal *P*6/*mmm* cell of the same volume. An attempt to relax the position of Pd ions in the *Cmmm* cell resulted in a small increase of the *y* positional parameter from 1/3 to 0.342 and a corresponding increase of the shortest U-Pd distance. The total energy gain from the relaxation is, however, much smaller than the energy difference between the orthorhombic and hexagonal structures. The doubling of the orthorhombic unit cell in the *c* direction and lowering of the symmetry to *Pmmm* would allow for the additional relaxation of Al positions and might make the orthorhombic structure more stable than the hexagonal one. We have to point out, however, that the calculations were performed using the atomic sphere approximation and, thus, cannot be considered as a decisive argument when comparing the relative stability of different crystal structures.

IV. DISCUSSION

A. Delocalization: Experimental approach

One important parameter to characterize the uranium electronic properties and delocalization phenomena is the evolution of its actual valence as a function of pressure. The estimation of the 5*f* charges in the uranium heavy fermion compounds remains, in fact, by far undetermined. We have already mentioned in the Introduction the difficulty to predict correctly the valent state or *f*-electron charge in UPt_3, UPd_3, and UPd_2Al_3, often leading to contradictory results. Experimentally, estimation of the valence is commonly obtained by measuring the chemical shift of the x-ray absorption spectra. However, in the uranium compounds, this method when applied to the L_3 edges turns out to be highly unreliable, in part, because the DOS in this energy region is dominated by the *d* states.

Unfortunately here, RIXS cannot provide a direct estimate of the U valency in the absence of isolated excitations which we could relate to the *f* states. However, the quality of our XAS spectra allows us to extract elements of information which are of importance in that context. Previous works have shown that simple quantities such as the white line maximum energy (E_{max}) and its half width at half maximum Γ exhibit a great sensitivity to the U-U distance and indirectly to the *f* hybridization and screening.[34,35] Figure 6 illustrates the variation of E_{max} and Γ in UPd_3 and UPd_2Al_3 with increasing pressure. Γ was estimated from the distance in energy between E_{max} and the Fermi energy (E_F, also shown in the figure), measured at the first inflection point of the absorption edge. UPd_3 and UPd_2Al_3 show strikingly different behaviors which reflect the opposite spectral changes. In UPd_2Al_3, Γ and E_{max} are mostly constant at low pressure while they mark a sudden step at the transition pressure P_C. Note that part of the linewidth broadening in UPd_2Al_3 could originate from saturation effects of the white line due to self-absorption. The results in UPd_3 demonstrate nevertheless that Γ and E_F do not change with pressure which would not be the case if self-absorption was strongly pressure dependent. As a further confirmation, we observe in UPd_2Al_3 similar trends in the pressure variations of E_F and Γ, which both depend on the saturation of the white line, and E_{max} a quantity independent of self-absorption since peak positions are conserved. The overall behavior can be reasonably attributed to the growth of the 6*d* bandwidth at shorter interatomic distance in agreement with the calculation. In addition, the more efficient screening of the core hole at higher density will tend to further enhance the electron delocalization as pressure increases. The pressure dependence $E_F(P)$ is more likely related to the white line broadening than to a change of the uranium valence state (in the chemical shift sense). Inversely, in UPd_3, these three parameters barely vary with

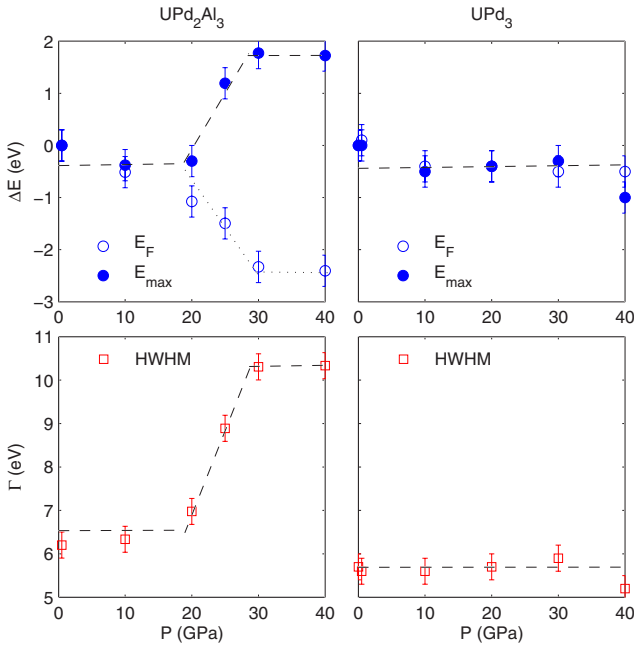

FIG. 6. (Color online) Estimated variation ΔE of the Fermi energy (E_F) (open circles) and white line position (E_{max}) (solid circles) with respect to the ambient pressure condition (upper panels) and half width at half maximum (Γ) (squares) (lower panels) for UPd_3 and UPd_2Al_3 as a function of pressure. Lines are guides to the eyes.

pressure. The result bears out the stability of the uranium electronic states with pressure—a comparable result was indirectly observed by EXAFS in UPd_3 upon chemical doping[36]—although the calculations do indicate a modest broadening of the 6*d* bandwidth and a slight positive shift of E_{max} that are not confirmed here. This phenomenological approach although informative does not account for the fine changes in the DOS with pressure especially in the main peak region.

B. Calculated U *f* charges

We propose now to derive the uranium electronic charges from the LMTO calculations. In our calculations, however, the ratio of the U and Pd (and Al) AS radii was kept constant with varying lattice parameters. Consequently, the radii themselves change with the decrease of the unit cell volume. Since in the LMTO ASA method site- and *l*-resolved charges are calculated as integrals of the electron density of appropriate symmetry over an atomic sphere, the direct comparison of the U 5*f* charges q_f^{U} obtained from calculations with different lattice constants becomes meaningless. When discussing the U 5*f* occupation, another problem arises because of the so-called "tails" of the states centered on neighboring sites that have the *f* character inside a uranium atomic sphere. The tails of Pd 4*d* states, for instance, contribute to the net U 5*f* charge but their contribution to the radial distribution of the *f*-electron density $\rho(r)$ increases as *r* approaches the sphere boundary in contrast to atomiclike U 5*f* states whose radial density has a maximum at ~0.6 Å.

In order to make a quantitative estimate of the pressure dependence of the U 5*f* occupation, we have extended our initial calculations with calculations for $ThPd_3$ and $ThPd_2Al_3$ performed using the same structural data and AS radii as for the corresponding uranium compounds. In both compounds, the Th 5*f* states are unoccupied, the peak of $5f_{5/2}$ DOS being located ~2 eV above the Fermi level. Thus, the 5*f* charge inside a Th sphere (q_f^{Th}) can be used as an estimate of the contribution of the tails of Pd and Al states to the U 5*f* charge and the occupation of the U 5*f* shell can be defined as the difference $\delta q_f = q_f^{\mathrm{U}} - q_f^{\mathrm{Th}}$. The effective U 5*f* occupation defined in this way shows only minor dependence on AS radii used in the calculations. It is interesting to note that by construction, δq_f is related to the localized *f* states, while q_f^{Th} rather points to the delocalized counterpart.

As it was discussed in Ref. 32 for UPd_3 at ambient pressure, the calculated 5*f* charges of two inequivalent uranium ions are 2.99 and 3.03. The 5*f* charge in corresponding Th atomic spheres is equal to 0.96 so that the average δq_f is 2.05, which is very close to the f^2 configuration expected for UPd_3.

The calculated pressure dependences of the *f* charges inside U and Th atomic spheres and $\delta q_f(P)$ for UPd_3 and UPd_2Al_3 are shown in Fig. 7. In both compounds, the *f* charge inside a U atomic sphere increases with pressure [Figs. 7(b) and 7(c)]. However, because of the more rapid increase of the delocalized *f* charge calculated for the corresponding Th compounds, the occupation of localized U 5*f* states δq_f decreases with the lattice compression.

In UPd_3, the occupation of the localized U 5*f* states averaged over two inequivalent uranium sites monotonously decreases from 2.05 at ambient pressure to 1.98 at 40 GPa. In the whole pressure range, δq_f remains very close to 2, which suggests that the valence state of U ions does not change under lattice compression. Thus, the picture that emerges is that of a localized f^2 configuration, consistent with the diffraction data of Ref. 18 and former band calculations by Ito *et al.*[15] Our finding definitively rules out the prediction of an f^2 to f^1 transition under pressure reported in Ref. 16.

In UPd_2Al_3 at ambient pressure, $\delta q_f = 2.17$, which indicates that the uranium ion is in an intermediate valence state. As the pressure increases up to P_C, δq_f decreases but at a somewhat higher rate than in UPd_3. Because of stronger compressibility of the *Cmmm* phase, the U 5*f* states depopulate even more rapidly above P_C and at $P > 33$ GPa, δq_f becomes less then 2. The kink in the δq_f plot at $P = 23.5$ GPa is attributed to the uncertainty in the experimental crystal structure at the critical pressure. The lattice parameters at this pressure were determined assuming the hexagonal unit cell. However, the cell volume of 86.83 $Å^3$ is smaller than the volumes of the *Cmmm* cell at 26.1 and 28.5 GPa (88.89 and 88.46 $Å^3$, respectively). This indicates that already at $P = 23.5$ GPa, both low and high pressure phases may coexist. Comparing the UPd_2Al_3 data to the $\delta q_f(0) = 2.05$ for UPd_3, for which the U $5f^2$ configuration is well established, one can suppose that the structural transition at $P_C = 23.5$ GPa is related to the change of the valence state of a uranium ion from an intermediate $U^{(4-\delta)+}$ valency to U^{4+}. This semiquantitative analysis does not allow us to answer the question whether the uranium valency in the HP

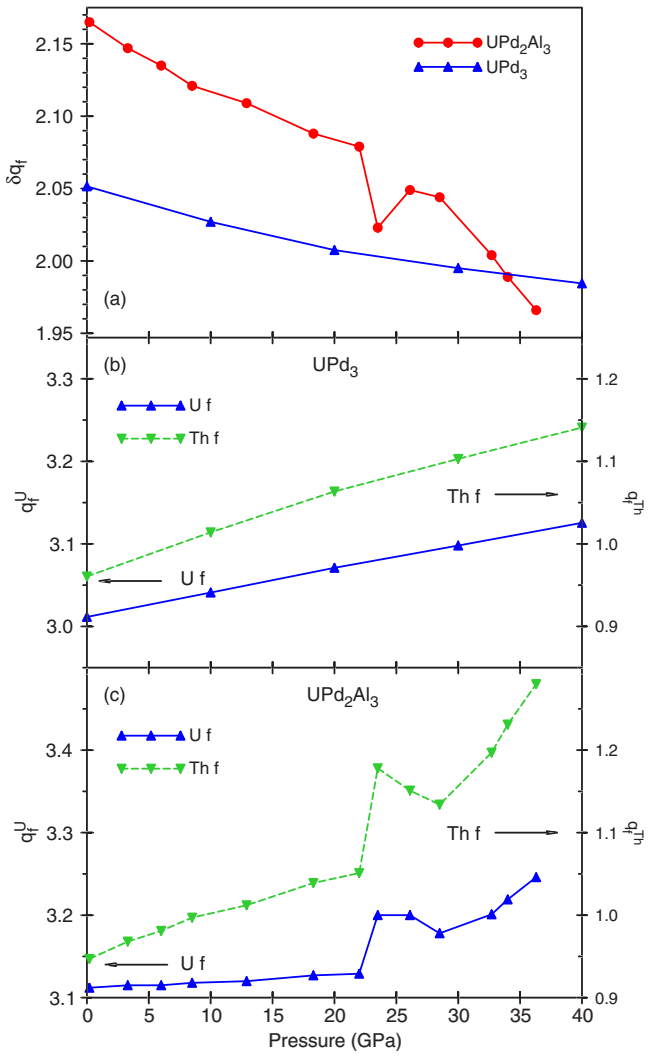

FIG. 7. (Color online) (a) The calculated pressure dependences of $\delta q_f = q_f^{\mathrm{U}} - q_f^{\mathrm{Th}}$ for UPd_3 (triangles) and UPd_2Al_3 (circles). For UPd_3, the U $5f$ occupation is averaged over the two inequivalent sites. The variation of the calculated f charges inside U and Th atomic spheres in U(Th)Pd_3 and U(Th)Pd_2Al_3 is shown in panels (b) and (c), respectively. Solid and dashed lines are interconnecting lines between points.

phase remains integer or becomes $U^{(4+\delta)+}$. It nevertheless agrees with the current understanding of the uranium valence in UPd_2Al_3 which is described by a coexistence of localized and delocalized f electrons. The intermediate valent state already formed at ambient pressure deviates from the precedent assumption of two localized and one delocalized f electrons.[37] It also contradicts bulk transport and magnetometric measurements that suggest tetravalency at ambient pressure[38] but without the atomic selectivity of RIXS.

It is worth mentioning that in UPd_3, the density of states at and down to ~1 eV below the Fermi level is very low and the Th $5f$ charge is provided by the tails of deep-lying Pd $4d$ states.[32] In $ThPd_2Al_3$, however, the Th $5f$ charge of about 0.3 electrons is accumulated within 1 eV below E_F. The rather high density of the Th $5f$ states in this energy range is due to the tails of Al $3p$ states hybridized with Pd $4d$ and $5s$ ones. As a consequence, δq_f in UPd_2Al_3 is more sensitive to a detailed charge balance between U $5f$ and delocalized Al $3p$ derived states.

Finally, the comparison of the U $5f$ DOS calculated for different pressure values shows that in both compounds, their width increases by only ~0.2 eV when the highest pressure is applied. Thus, the $5f$ bandwidth remains smaller than the typical values of 2–2.5 eV for the Coulomb parameter U for U $5f$ electrons and the strong electronic correlations are important even under high pressure.

V. CONCLUSION

The pressure-induced electron delocalization phenomena were investigated in UPd_3 and UPd_2Al_3 by RIXS-derived spectroscopic techniques. More particularly, we have focused on the variation of the U L_3 absorption spectra, measured in the partial fluorescence yield mode, as a function of pressure. In this context, RIXS has several advantages. It is a bulk probe fully compatible with the high pressure sample environment; RIXS is selective of the atomic orbitals, while the spectral sharpening which results from the second-order scattering type yields data of superior quality. This in turn largely facilitates their interpretation. By comparing the experimental results with LMTO calculations, one can now understand how the f-d states are modified in the compressed lattice. In both samples, we observe a sizable widening of the $6d$ band directly related to the shortening the interatomic distances as pressure increases. More interestingly, the f electrons are found to remain largely localized in UPd_3 over the entire pressure range, whereas in UPd_2Al_3 we observe a significant decrease of the f electronic charge under pressure, while preserving strong correlation. This valence change is likely at the origin of the structural instability at high pressure. The results are in stark contrast with recent SIC-LSD calculations,[16] calling for a renewed theoretical description of the strongly correlated uranium compounds.

ACKNOWLEDGMENTS

We acknowledge A. Krimmel for providing us with unpublished preliminary data on the high pressure phase of UPd_2Al_3 and J.-P. Sanchez for critical reading of the manuscript.

[1] J. Flouquet, *On the Heavy Fermion Road*, Progress in Low Temperature Physics Vol. 15 (Elsevier, New York, 2005), Chap. 2 and references therein.
[2] A. Holmes, D. Jaccard, and K. Miyake, Phys. Rev. B **69**, 024508 (2004).
[3] P. P. Deen, D. Braithwaite, N. Kernavanois, L. Paolasini, S. Raymond, A. Barla, G. Lapertot, and J.-P. Sanchez, Phys. Rev. B **71**, 245118 (2005).
[4] E. Annese, A. Barla, C. Dallera, G. Lapertot, J.-P. Sanchez, and G. Vankó, Phys. Rev. B **73**, 140409(R) (2006).
[5] C. Dallera, M. Grioni, A. Shukla, G. Vankó, J. L. Sarrao, J.-P. Rueff, and D. L. Cox, Phys. Rev. Lett. **88**, 196403 (2002).
[6] C. Dallera, E. Annese, J.-P. Rueff, A. Palenzona, G. Vankó, L. Braicovich, A. Shukla, and M. Grioni, Phys. Rev. B **68**, 245114 (2003).
[7] C. Dallera, M. Grioni, A. Palenzona, M. Taguchi, E. Annese, G. Ghiringhelli, A. Tagliaferri, N. B. Brookes, T. Neisius, and L. Braicovich, Phys. Rev. B **70**, 085112 (2004).
[8] J.-P. Rueff, C. F. Hague, J.-M. Mariot, L. Journel, R. Delaunay, J.-P. Kappler, G. Schmerber, A. Derory, N. Jaouen, and G. Krill, Phys. Rev. Lett. **93**, 067402 (2004).
[9] E. Annese, J.-P. Rueff, G. Vankó, M. Grioni, L. Braicovich, L. Degiorgi, R. Gusmeroli, and C. Dallera, Phys. Rev. B **70**, 075117 (2004).
[10] C. Dallera, E. Annese, J.-P. Rueff, A. Palenzona, G. Vankó, L. Braicovich, A. Shukla, and M. Grioni, J. Electron Spectrosc. Relat. Phenom. **137-140**, 651 (2004).
[11] C. Dallera *et al.*, J. Phys.: Condens. Matter **17**, S849 (2005).
[12] J.-P. Rueff, J.-P. Itié, M. Taguchi, C. F. Hague, J.-M. Mariot, R. Delaunay, J.-P. Kappler, and N. Jaouen, Phys. Rev. Lett. **96**, 237403 (2006).
[13] G. H. Lander, M. S. S. Brooks, and B. Johansson, Phys. Rev. B **43**, 13672 (1991).
[14] W. J. L. Buyers and T. M. Holden, *Handbook on the Physics and Chemistry of the Actinides* (Elsevier, New York, 1987), p. 289.
[15] T. Ito, H. Kumigashira, S. Souma, T. Takahashi, Y. Haga, Y. Tokiwa, and Y. Onuki, Phys. Rev. B **66**, 245110 (2002).
[16] L. Petit, A. Svane, W. M. Temmerman, and Z. Szotek, Phys. Rev. Lett. **88**, 216403 (2002).
[17] W. M. Temmerman, A. Svane, Z. Szotek, and H. Winter, *Electronic Density Functional Theory: Recent Progress and New Directions* (Plenum, New York, 1998).
[18] S. Heathman, M. Idiri, J. Rebizant, P. Boulet, P. S. Normile, L. Havela, V. Sechovský, and T. Le Bihan, Phys. Rev. B **67**, 180101(R) (2003).
[19] J. W. Allen, *Resonant Photoemission of Solids with Strongly Correlated Electrons*, Synchrotron Radiation Research: Advances in Surface and Interface Science Vol. 1 (Plenum, New York, 1992), Chap. 6, p. 253.
[20] G. Zwicknagl, A. N. Yaresko, and P. Fulde, Phys. Rev. B **65**, 081103(R) (2002).
[21] G. Zwicknagl and P. Fulde, J. Phys.: Condens. Matter **15**, S1911 (2003).
[22] A. Krimmel, A. Loidl, K. Knorr, B. Buschinger, C. Geibel, C. Wassvilew, and M. Hanfland, J. Phys.: Condens. Matter **12**, 8801 (2000).
[23] G. Fiquet and B. Reynard, Am. Mineral. **84**, 856 (1999).
[24] P. Dalmas de Réotier, A. Yaouanc, G. van der Laan, N. Kernavanois, J.-P. Sanchez, J. L. Smith, A. Hiess, A. Huxley, and A. Rogalev, Phys. Rev. B **60**, 10606 (1999).
[25] A. Yaouanc, P. D. de Réotier, G. van der Laan, A. Hiess, J. Goulon, C. Neumann, P. Lejay, and N. Sato, Phys. Rev. B **58**, 8793 (1998).
[26] K. Hämäläinen, D. P. Siddons, J. B. Hastings, and L. E. Berman, Phys. Rev. Lett. **67**, 2850 (1991).
[27] F. M. F. de Groot, M. H. Krisch, and J. Vogel, Phys. Rev. B **66**, 195112 (2002).
[28] J.-P. Rueff, L. Journel, P.-E. Petit, and F. Farges, Phys. Rev. B **69**, 235107 (2004).
[29] P. Carra, M. Fabrizio, and B. T. Thole, Phys. Rev. Lett. **74**, 3700 (1995).
[30] M. O. Krause and J. H. Oliver, J. Phys. Chem. Ref. Data **8**, 329 (1979).
[31] D. A. Zatsepin, S. M. Butorin, D. C. Mancini, Y. Ma, K. E. Miyano, D. K. Shuh, and J. Nordgren, J. Phys.: Condens. Matter **14**, 2541 (2002).
[32] A. N. Yaresko, V. N. Antonov, and P. Fulde, Phys. Rev. B **67**, 155103 (2003).
[33] A. Krimmel (private communication).
[34] J. M. Lawrence, M. L. den Boer, R. D. Parks, and J. L. Smith, Phys. Rev. B **29**, 568 (1984).
[35] G. Kalkowski, G. Kaindl, W. D. Brewer, and W. Krone, Phys. Rev. B **35**, 2667 (1987).
[36] M. Akabori, T. Ogawa, A. Itoh, H. Motohashi, and H. Shiwaku, J. Alloys Compd. **271-273**, 363 (1998).
[37] L. Petit, A. Svane, W. M. Temmerman, Z. Szotek, and R. Tyer, Europhys. Lett. **62**, 391 (2003).
[38] A. Grauel *et al.*, Phys. Rev. B **46**, 5818 (1992).